

Original Article

# Influence of Damping on the Seismic Response of High-Rise Reinforced Concrete Buildings

Víctor Hinostroza Maraví<sup>1\*</sup>, Benjamin De la Cruz Taipe<sup>1</sup>, Jean Fernando Pérez Montesinos<sup>2</sup>

<sup>1</sup>Department of Civil Engineering, Universidad Continental, Huancayo, Junin.

<sup>2</sup>School of Civil Engineering, University of Idaho, Idaho, USA.

<sup>1</sup>Corresponding Author : 75476788@continental.edu.pe

Received: 16 October 2025

Revised: 20 January 2026

Accepted: 29 April 2026

Published: 29 May 2026

**Abstract** - Recent earthquakes have highlighted that, in addition to their strength, the seismic resistance of reinforced concrete buildings is related to their ability to dissipate energy (damping). In engineering practice, the most common approach for the critical damping in dynamic analysis is to consider a reference value of 5% in building codes, but some experimental and analytical research have shown that the real values in reinforced concrete buildings often have a damping ratio in the range of 2% and 3%. This may result in an underestimation or overestimation of the seismic demand, affecting the safety and economic aspects of the structure. This paper aims to determine the effect of the damping ratio on the seismic performance of reinforced concrete buildings, considering the 5% normative as a reference. A numerical study was conducted with ETABS software for a 17-floor and 4-basement level building in Lima, Peru. The structure was modelled as a reinforced concrete shear wall, with overall damping ratios set at 2%, 3%, 4% and 5%. Loads were evaluated considering the E.020 code (gravitational loads) and E.030 code (seismic loads), using the modal response spectrum, with accidental eccentricities in both directions. It was found that decreasing the damping ratio from 5% to 2% caused substantial increases in structural response. Displacements increased from 252 mm to 310 mm, interstory drift from 0.0053 to 0.0066, and base shear from 632 tonf to 805 tonf, with the largest changes in the Y-axis. The results verified the effects of changing the damping ratio on the seismic response and also demonstrate the need to use more realistic values. The findings of this research offer quantitative data that can inform seismic design practices in order to improve safety and economy. The main weakness of this research is that the analyses were linear and only one building typology was considered; for this reason, future studies should consider nonlinear analyses and other structural typologies, increasing the generalisation potential of these findings.

**Keywords** - Reinforced concrete buildings, Seismic damping, Structural response, Interstory drift, Base shear.

## 1. Introduction

Peru is highly susceptible to earthquakes. It is located on the Pacific Ring of Fire, next to Chile, where 80% of the world's earthquakes take place. This is because it is close to the Nazca and South American tectonic plates. However, such events can happen in any seismically active country, such as the February 2023 earthquake in Turkey, and have demonstrated that for a reinforced concrete building to be safe, it is not enough that it is strong. It must also dissipate earthquake energy, which is provided by damping [1, 2]. In practice, most building codes use a constant value of 5% damping as a reference in dynamic analyses [3, 4]. However, this simplistic approach to model damping does not take into account the complicated energy dissipation mechanisms of a structure during the earthquake [5, 6]. Some recent research has demonstrated that if the value of damping adopted for the standard design is not equal to the value of damping that the structure would actually have, the seismic demands of the structure can be underestimated. This can result in designs that

are unsafe or, on the contrary, unnecessarily expensive. This has obvious implications on both safety and construction/repair costs [7, 8].

Although the damping ratio is usually very similar, between 1% or 2% differences can substantially change the vibration response of a structure during an earthquake. This has an impact on inter-story drifts and forces, which in turn affect the design quality and safety levels [9, 10]. In this sense, the proper evaluation of damping, which is closely related to material stiffness, is a key technical issue to ensure the adequacy of seismic design, and an economic factor to avoid overdesign and post-earthquake damages [11-13].

The state of the art reflects intense research activity focused on the characterization of damping. Experimental studies have demonstrated the interdependence between stiffness and energy dissipation, while advanced methodologies such as Random Decrement Technique (RDT)



combined with statistical approaches have been developed to quantify uncertainty [14, 15]. Other research has employed ambient vibration records in instrumented buildings to estimate dynamic properties [16]. In terms of reported values, damping in reinforced concrete structures is often found to range between 2% and 3% [17, 18], in masonry systems around 3%, while non-structural elements such as partitions or infill walls also exert additional influence [19-21].

In addition, damping adjustment factors have been proposed that vary according to the type of soil and the time it takes for the structure to oscillate. In other words, they do not apply equally in all cases, but depend on the site conditions and the dynamic behavior of the building. [22]. Despite the progress that has been made, it is not yet fully understood how these variations influence the results provided by commercial structural analysis programs. Some studies have indicated that reducing the assumed default damping value increases the design requirements and may affect the overall seismic performance of the structure. [23].

Conversely, another study [19] conducted at an educational facility in Peru with damping ratios ranging from 2% to 5% revealed that using a damping ratio of 2% resulted in floor-to-floor deflections increasing by 15–32% and internal stresses in the structure increasing by 6–24%, representing significant increases. Furthermore, the relatively conventional damping value of 5% is used in various cases to evaluate the interaction between frames and infill walls [22].

In this study, models of reinforced concrete buildings created in ETABS software [24] were used to analyze how different damping values affect the seismic response. In the case of this study, the normative value of 5 % was taken as a reference and then compared with reduced values of 2 %, 3 %, and 4 %. With regards to the analysis, it was focused on crucial parameters, like the lateral displacements, inverstory drifts, base shear, and overturning moments.

**2. Materials and Methods**

The approach taken in this research started with defining the structural model, then assigning seismic loads, and then varying the damping ratio so the impact on the overall performance of the building could be quantified [25]. The study focuses on analyzing the dynamic behavior of buildings of different heights. We change the values of the ratio of the two types of springs that work together to make the building stable. This is done to make the building safer. However, we are not studying a very complex situation. We are studying only a simple situation. This is because we need to know how much reinforcement is needed. This information would be useful for other situations. In this case, the E.030 standard was used, which includes this type of analysis (see Table 1). This analysis is used to determine the applicability to these structural types.

**2.1. Building Description**

The construction studied in this paper was a reinforced concrete structure that is located in the department of Lima, Peru. It has 17 above-ground stories and 4 basement levels. The structural system has reinforced concrete walls as its main component, which goes in line with the classification that was established by the Technical Standard E.030 [26]. This standard secures an adequate lateral stiffness that withstands the high seismic rate and demand of the region. The dimensions of the basement are the following: 24.6 m in the X direction and 31.5 m in the Y direction, although the upper stories keep 24.6 m in X and 26.4 m in Y axes.

The floor has a L-shape configuration that makes the building be classified as an irregular one because of a re-entrant corner, according to the Peruvian seismic-resistant code [26]. This L-shape attribute of this building causes an increment in the complexity of the structural analysis, since it introduces additional torsional effects that have an impact on the stress distribution and displacements. Different types of concrete were considered for the modeling purposes, and their mechanical properties, such as the compressive strength, the modulus of elasticity, and the unit weight, are summarized and shown in Table 1.

**Table 1. Mechanical properties of the materials used in the analysis**

Material	Resistance	Modulus of Elasticity	Unit Weight
Concrete 1	$f'c = 28$ Mpa	23,800 MPa	24.0 kN/m
Concrete 2	$f'c = 35$ Mpa	26,500 MPa	24.0 kN/m
Reinforcement Steel	$fy = 420$ Mpa	200,000 MPa	78.5 kN/m

Figure 1 depicts the three materials that were analyzed. Concrete 2 was employed in the basements and in the first six stories of the building, while from the seventh floor to the top floor, Concrete 1 was utilized. This configuration was decided because of the structural design criteria that state that the lower levels require a higher-strength concrete to adequately react to both the high vertical load demands and the seismic forces concentrated at the base.

Regarding the upper levels, lower-strength concrete was used because it permitted optimizing the employment of materials, and also it avoided affecting the safety or the overall performance of the structure. In addition, different horizontal elements (beams, slabs, and stairs) were modeled using Concrete 1; in this way, uniformity in the characterization of these structural components could be warranted. In the figure, Concrete 2 was represented by the black color, while Concrete 1 was represented by the gray color. This approach eased the visual differentiation of the materials in the model.

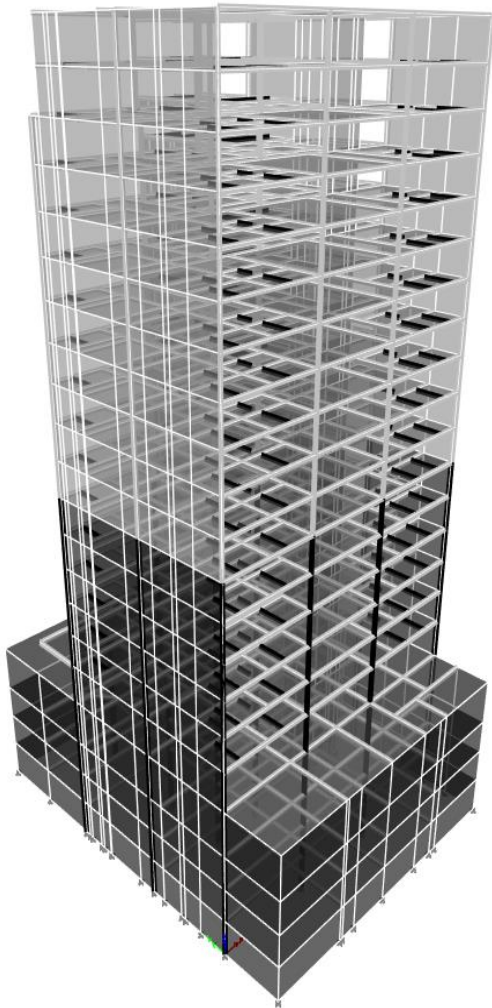


Fig. 1 Distribution of materials in the analyzed building

Figure 2 portrays the structural configuration of the basements, while Figure 3 depicts the structural configuration of the typical floors. This exemplification allows us to identify the wall distribution and the spatial organization of the resisting system. The cornerstone of the numerical analysis in this paper is these representations because they show the actual geometry of the building, and they also highlight the arrangement of the load-bearing elements, which condition the behavior of the construction under seismic loads. The basement construction drawing manifests a regular layout that was designed to endure the high demands of the lower levels. Meanwhile, the typical floor plan has an L-shaped configuration, and this is classified as a re-entrant corner irregularity according to Technical Standard E.030 [26]. The circumstances of these buildings introduce additional torsional effects that not only increase the complexity of the analysis, but also make a detailed modeling that is more than necessary to accurately appraise the structural response when put under different damping scenarios. Also, the walls of relleno in the reinforced concrete structure were not

considered because they do not support the structure. For the model, they were considered dead load. As you know, these walls are separated from the structure during construction with joints to prevent damage to the structure and to prevent distorting the natural frequencies and floor-to-floor distortions [26].

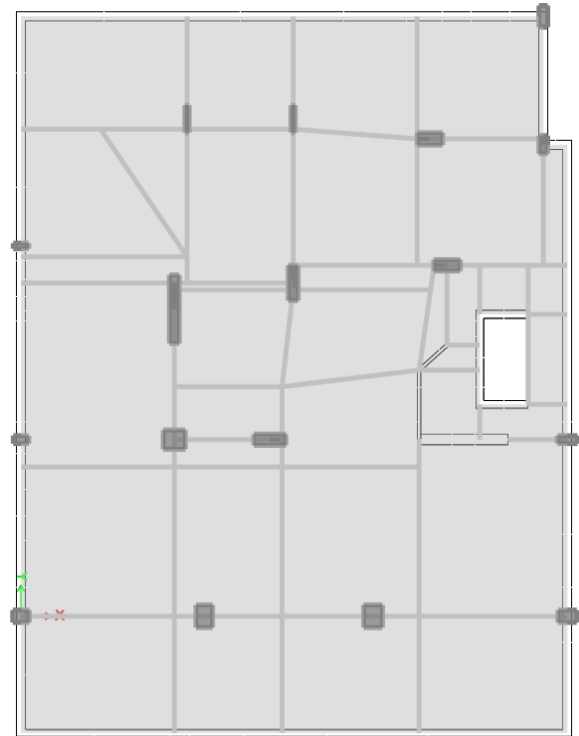


Fig. 2 Structural configuration of the basements

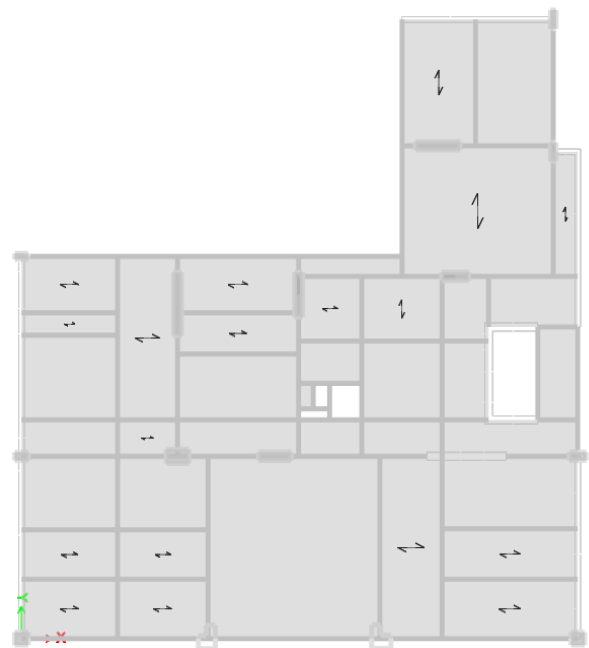


Fig. 3 Structural configuration of the typical L-shaped floors

**2.2. Modeling in ETABS**

For the performance of the structural analysis, the ETABS software was employed [24] while considering the actual geometry of the building, which has 17 stories and 4 basements. The materials chosen for this analysis were defined according to the properties shown in Table 2, assigning sections to each structural element. The slabs were modeled as membrane elements, the walls as shell elements, and the beams and columns as frame elements. This decision allowed us to do an adequate representation of the global behavior of the building.

With regards to the seismic mass, it was obtained from the self-weight and additional dead loads, respecting the Technical Standard E.030 [26]. The damping characteristic was assigned globally with values of 2%, 3%, 4%, and 5%, in order to evaluate its influence on the structural response. Finally, load combinations defined in the Peruvian seismic-resistant code were applied, so the consistency in the analysis procedure could be ensured.

**2.3. Loads and Boundary Conditions**

The gravitational loads were defined according to the Technical Standard E.020 [27], and they corresponded to a

Residential building of category C. The self-weight of the structural elements and the additional dead loads associated with both the finishes and the coverings were considered. Considering the live loads, these were assigned according to the occupancy, differentiating three areas: the habitable, the circulation, and the parking spaces.

The seismic loads were determined considering the Technical Standard E.030 [26], and the regulatory parameters corresponding to Lima were also taken into account.

These values include the Zone Factor (Z), Soil Factor (S), Use Factor (U), Seismic Amplification Factor (C), and Ductility Reduction Factor (R); all these factors are summarized in Table 2. Based on these parameters, the design spectrum used in the dynamic analysis was constructed.

Regarding the boundary conditions, the vertical elements were considered as fixed at the base, with the goal of ensuring the proper transmission of forces to the foundation. It is important to note that these values are based on a 10% chance of failure over 50 years, which is the same as a 475-year return period [26].

**Table 2. Mechanical properties of the materials used in the analysis**

Parameter	Symbol	Valor	Description
Zone Factor	Z	0.45	It corresponds to the city of Lima, a high-seismicity zone
Soil Factor	S	1.00	Intermediate soil type S1 according to the standard classification
Use Factor	U	1.00	Category C building – Residential
Seismic amplification factor	C	2.50	Maximum value in the range of intermediate periods
Reduction factor	R	6.00	Associated with a reinforced concrete wall structural system

**2.4. Linear Dynamic Analysis**

The linear dynamic analysis procedure was carried out by using the modal superposition method, which permitted the guarantee that the accumulated modal participation reached at least 90% of the mass in both principal directions, in accordance with Technical Standard E.030 [26]. Later on, the modal combination was performed by applying the Square Root of the Sum of Squares (SRSS) method for independent modes and the Complete Quadratic Combination (CQC) method when modal coupling was present.

The Damping aspect was implemented through the Rayleigh formulation, which is expressed as a linear combination of the mass matrix [M] and the stiffness matrix [K], as depicted in Equation 1. This approach, which is widely used in structural software, enables the assignment of an energy dissipation level based on the most representative vibration modes of the structure [28].

$$C = \alpha M + \beta k \tag{1}$$

The damping coefficients  $\alpha$  and  $\beta$  were calculated based on two selected natural frequencies, ensuring that the critical damping ratio  $\zeta$  adopted the desired values in the modes of interest, as expressed in Equation 2 [28].

$$\zeta = \frac{1}{2} \left( \frac{\alpha}{\omega} + \beta \omega \right) \tag{2}$$

The representation of damping in the model was established as a fundamental aspect of the linear dynamic analysis. For this purpose, global ratios of 2%, 3%, 4%, and 5% were employed. This includes the ranges of the damping ratio, which depends on the material and the service load condition (SLS) or the ultimate load condition (ULS) that the structure experiences under dynamic loading [29]. As shown in Table 3, it was implemented through the Rayleigh

formulation. Figure 4 includes a schematic of an SDOF system subjected to free vibration, which was used as an illustrative resource to graphically show the effect of different damping levels on energy dissipation.

Table 3. Values for the damping ratio

Estado	Condicion de estructura	Damping Ratio (%)
SLS	Well – reinforced concrete	2 - 3
	Reinforced concrete with considerable cracking	3 - 5

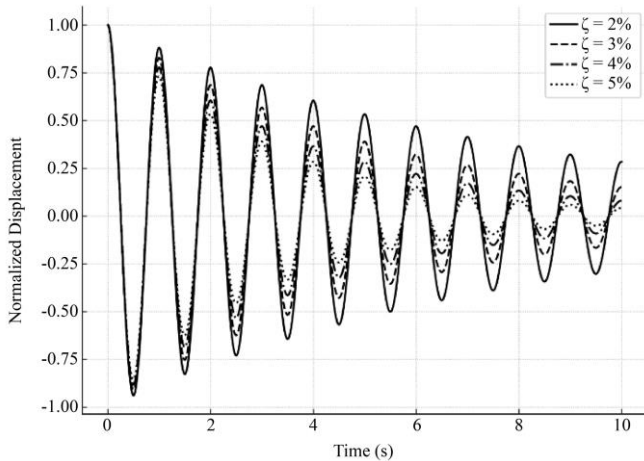


Fig. 4 Free Vibration Response of an SDOF System with Different Damping Ratios

### 3. Results

The results of the linear dynamic analysis are presented according to the parameters defined in the methodology, covering lateral displacements, interstory drifts, base shear, overturning moment, and floor accelerations. In each case, the different damping ratios established in the model and the eccentricity combinations applied in both principal directions were considered.

#### 3.1. Base Shear

Figure 5 shows the variation of base shear as a function of the damping ratio for the eccentricity cases in the X direction. In the DX scenario, the initial values at the base were 631.97 tonf with 5% damping and increased up to 805.41 tonf with 2%, while in the upper levels, a maximum of 3450.99 tonf was recorded in the same 2% scenario.

For DX+, the results followed a similar trend, with an increase from 649.02 tonf (5%) to 824.73 tonf (2%) at the base, reaching a maximum of 3520.26 tonf in the upper levels with 2%. These values show that, in the X direction, the reduction of damping produces progressive and sustained increases in base shear along the height of the building.

In the Y direction, the results were higher compared to the X direction. For DY-, the base shear increased from 737.12 tonf at 5% damping to 911.41 tonf at 2% at the base, reaching a maximum of 4591.21 tonf in the upper levels under the lowest damping scenario. In the case of DY+, the values ranged from 643.21 tonf (5%) to 801.91 tonf (2%) at the base, with a maximum of 4317.81 tonf recorded in the upper levels. Overall, the results confirm that reducing damping from 5% to 2% produced consistent increases in base shear in the four configurations analyzed, being more pronounced in the Y direction, especially in the DY scenario.

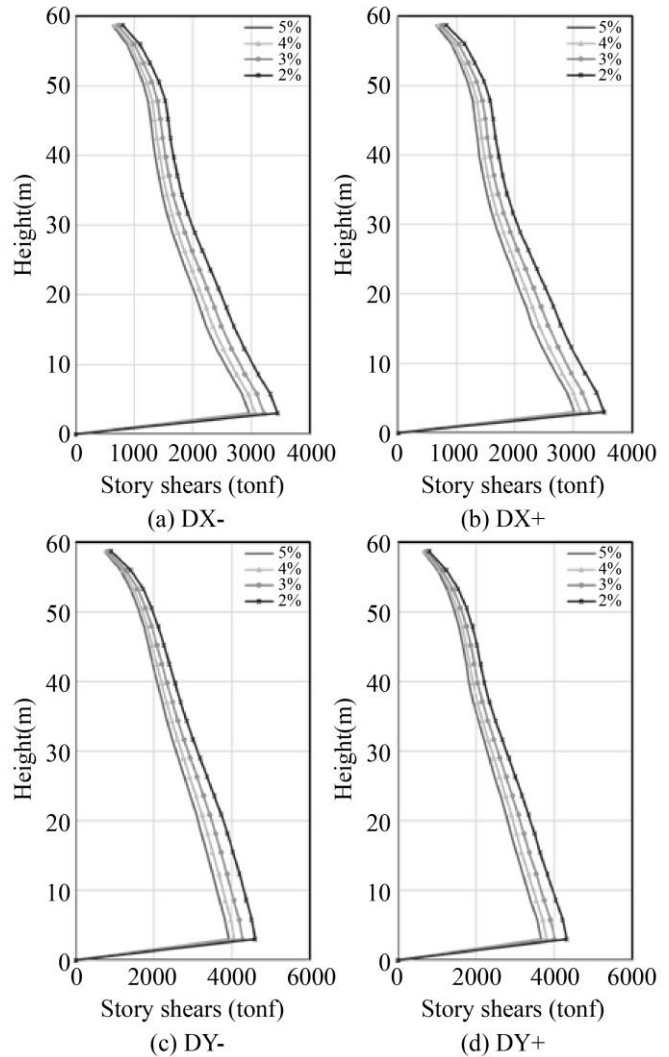


Fig. 5 Variation of base shear as a function of the damping ratio for the eccentricity cases

#### 3.2. Displacement

In Figure 6, the lateral displacements corresponding to the four eccentricity cases analyzed under damping ratios of 5%, 4%, 3%, and 2% are presented. In the X direction, case DX- reached a maximum displacement of 252.22 mm with 5% damping and 309.88 mm with 2%, while in DX+, the values

ranged from 242.43 mm (5%) to 297.92 mm (2%). In both scenarios, a progressive increase in displacements can be observed as the damping ratio decreases, with intermediate records of 266.29 mm (4%) and 284.40 mm (3%) in DX-, and 255.98 mm (4%) and 273.41 mm (3%) in DX+.

In the Y direction, lower values were obtained compared to the X cases. For DY-, the maximum displacement was 168.52 mm with 5% and 209.03 mm with 2%, while in DY+, the results ranged between 170.84 mm (5%) and 210.17 mm (2%). As in the previous cases, continuous increments were observed in the intermediate levels, with values of 178.61 mm (4%) and 191.38 mm (3%) in DY-, and 180.47 mm (4%) and 192.83 mm (3%) in DY+. These results confirm that the variation in damping consistently affects lateral displacements in all the eccentricity configurations considered.

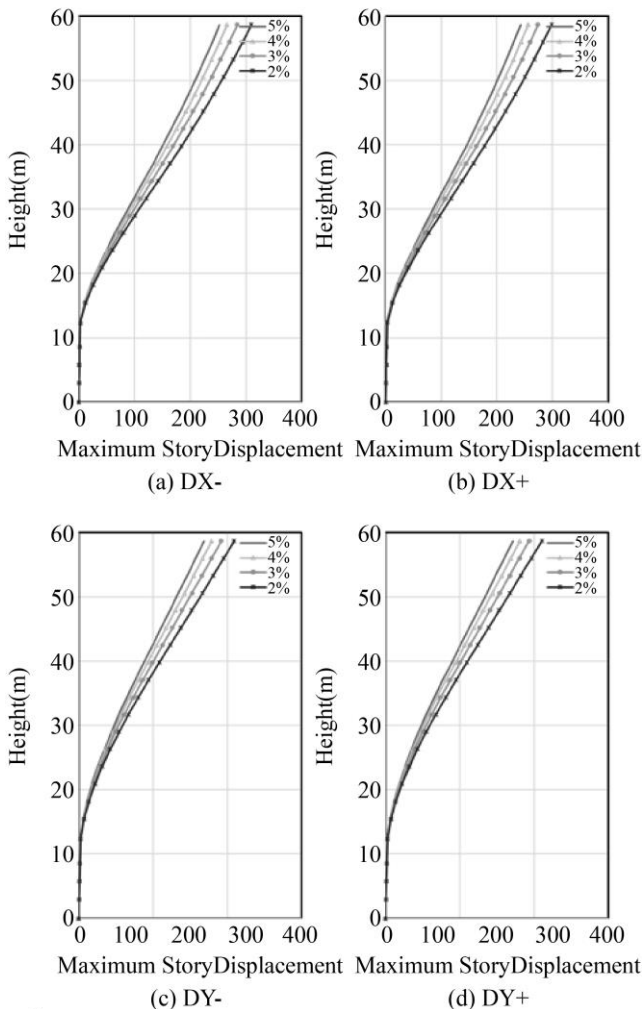


Fig. 6 Lateral displacements as a function of damping ratio for the eccentricity cases

### 3.3. Interstory Drift

Figure 7 presents the interstory drifts corresponding to the four eccentricity cases (DX-, DX+, DY-, and DY+) under damping ratios of 5%, 4%, 3%, and 2%. In the X direction, the

DX- case recorded an increase from 0.00534 with 5% damping to 0.00657 with 2% in the lower levels, reaching maximum values of 0.00820 in the mid-height region. In the DX+ case, the results evidenced that, by reducing the damping of the buildings from 5% to 2%, the drifts increased progressively along with the height of the constructions. The maximum value recorded at the upper levels was 0.00790. This increment was especially appreciable at the intermediate floors, where the effect of the damping reduction was most pronounced.

In the Y-axis, the interstory drifts were smaller than in the X-axis. In the case of DY-, the reduction of the damping from 5 % to 2 % increased the drift from 0.00429 to 0.00532, reaching a maximum of 0.00556 at intermediate levels. In the DY+ case, the values ranged from 0.00435 (at 5 % of damping) to 0.00535 (at 2 % of damping), with a maximum value of 0.00560. Generally speaking, the results obtained demonstrate a consistent behavior across the four eccentricity configurations, where a decrease in the damping that goes from 5% to 2% triggered gradual and systematic increases in interstory drifts.

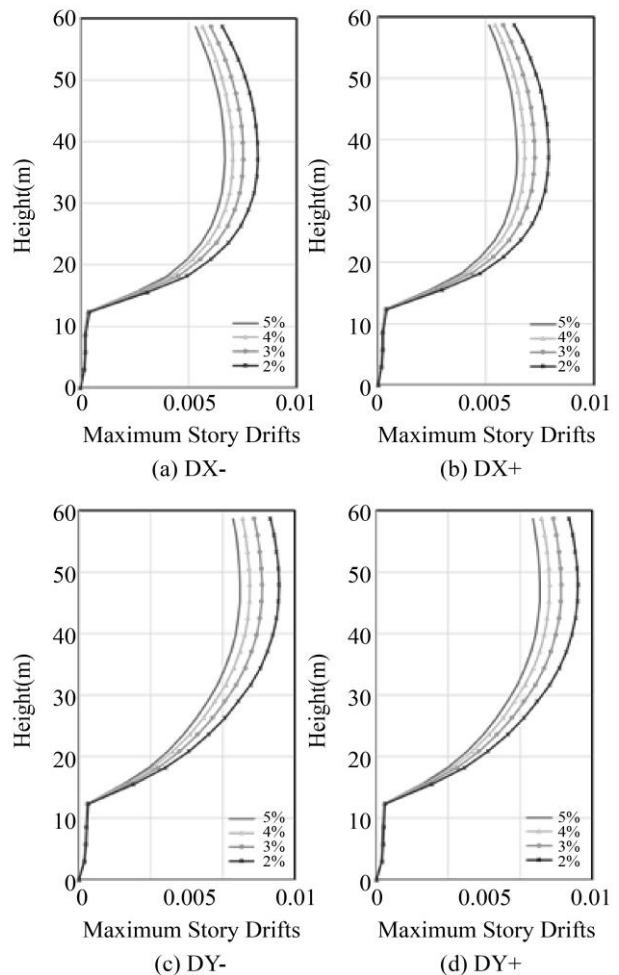


Fig. 7 Interstory drifts as a function of damping ratio for the eccentricity cases

#### 4. Discussion

All these results acquired show that the reduction of damping in infrastructures from the normative value of 5% to levels as low as 2% yields a steady increase in both displacements and interstory drifts, as well as in the base shear. This behavior demonstrates that the damping feature of buildings is a critical parameter in seismic energy dissipation and that small variations in it can substantially change the structural demand. In addition, these outcomes are consistent with recent research, and this showcases that the normative simplification of a single damping value does not always adequately represent the actual mechanisms of energy dissipation in reinforced concrete buildings [5, 7].

In this context, the sensitivity of the structural response observed in the analyzed models is in line with experimental and numerical studies that report that real damping values close to 2–3% in reinforced concrete structures are below the 5% commonly used in practice [17, 18]. The consistency between the present results and these previous studies underscores the necessity to reconsider the application of fixed normative values, particularly in high-rise buildings, where the effect of damping is closely linked to stiffness and the interaction with non-structural elements. In this regard, this present research provides quantitative evidence that invigorates the technical discussion on the importance of incorporating more realistic damping ranges in seismic analysis, which have direct implications not only for design accuracy but also for its economic optimization.

The studies based on actual cases in Japan [30] for an 8-story building using steel-encased reinforced concrete, and shake table tests on reinforced concrete structures and structural concrete walls in Mexico [31], suggest that the 2% damping ratio is the most common value in the overall behaviour. If you agree with the changes, the structural systems will be stronger. This will translate to higher internal stress and, as a consequence, will increase the material cost.

For an educational building, an inter-floor drift (in the direction "X") was found to be around 32% [19], while the increase in this study was of 24% (from 0.00534 to 0.00657). This is due to the building typology (reduction factor "R"). However, these tall buildings generally collapse at drift values of 3% or 4.5% [22]; in this case, the maximum drift is 0.82%, showing that there is a margin of energy dissipation to reach the capacity of the building.

Another important point is that the current standards E030 [26], ASCE/SEI 7-22 [32], and Eurocode [33] agree on the definition of the damping ratio for reinforced concrete (5%), but there is a discrepancy in the specific provisions of each. In the case of the Eurocode, the design spectrum is defined based on the damping ratio ( $\zeta$ ); ASCE/SEI 7-22 allows the ratio to be reduced to 2%–3% for high-rise buildings; however, the

Peruvian standard E.030 does not include specific provisions for these cases.

For tall buildings where the natural period is high, the variation in the damping ratio does not change much in the soil–structure interaction [33]. However, since this damping coefficient depends on amplitude, it increases in the following order: microtremors, forced excitation, and seismic observation. It was also found that the damping coefficient can decrease as the amplitude increases, as shown in Figure 8.

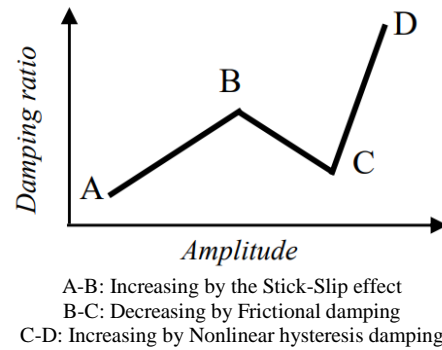


Fig. 8 Relationship between damping ratio and amplitude [34]

In recent years, there have been many types of dampers, but it is important to choose the correct one for the type of structure and the structure's size. In this case, the Viscous Fluid Damper (VFD) is the most appropriate to avoid hinges in reinforced concrete buildings [35].

#### 5. Conclusion

This research estimated the impact of changes in the damping ratio on the seismic behaviour of reinforced concrete buildings, using numerical models in ETABS. It was found that the reduction of the standard value of 5% to values of 2-3% lead to a progressive increase in the performance parameters of the structures, establishing the sensitivity of the models to this factor.

These findings offer quantitative insights into the need to review the use of a single value for damping in design codes, especially in the case of tall buildings. The study adds to the technical knowledge base by showing that small changes in this factor can lead to substantial changes in displacements, interstory drifts, and internal forces, which affect design and construction costs, both in the design phase and in improving the economic efficiency of building resources.

Finally, the findings of this study were obtained through linear analysis of a particular building case; it is suggested that additional studies should consider nonlinear analysis, different structural configurations, and non-structural elements to understand better the damping factor and its influence on the safety and reliability of seismic design.

## References

- [1] Chaofeng Liang et al., “Relationship between Internal Viscous Damping and Stiffness of Concrete Material and Structure,” *Structural Concrete*, vol. 22, no. 3, pp. 1410-1428, 2021. [[CrossRef](#)] [[Google Scholar](#)] [[Publisher Link](#)]
- [2] Vladimir Smirnov, and Michail Smolyakov, “Experimental Method for Structural Concrete Damping Properties Evaluation,” *International Journal for Computational Civil and Structural Engineering*, vol. 18, no. 4, pp. 14-22, 2022. [[CrossRef](#)] [[Google Scholar](#)] [[Publisher Link](#)]
- [3] EmreÇağlar Çelik, and Onur Merter, “An Investigation of Damping Modification Factors Corresponding to Different Damping Ratios for SDOF Systems,” *Civil Engineering Journal*, vol. 31, pp. 1-12, 2023. [[CrossRef](#)] [[Google Scholar](#)] [[Publisher Link](#)]
- [4] Stipe Perišić et al., “Automatic Damping Estimation via Bootstrap Technique and Bayesian Analysis for Mechanical System Condition Monitoring,” *Mechanical Systems and Signal Processing*, vol. 220, 2024. [[CrossRef](#)] [[Google Scholar](#)] [[Publisher Link](#)]
- [5] Mohammad Reza Khosravi et al., “A Study of Progressive Collapse in Moment-Resisting Reinforced Concrete Structures Considering Damping Ratio,” *Iranian Journal of Science and Technology, Transactions of Civil Engineering*, vol. 48, pp. 3323-3337, 2024. [[CrossRef](#)] [[Google Scholar](#)] [[Publisher Link](#)]
- [6] G. Rebecchi et al., “Full-Scale Shake Table Tests of a Reinforced Concrete Building Equipped with a Novel Servo-Hydraulic Active Mass Damper,” *Journal of Earthquake Engineering*, vol. 27, no. 10, pp. 2702-2725, 2023. [[CrossRef](#)] [[Google Scholar](#)] [[Publisher Link](#)]
- [7] Luca Verrucci et al., “Damping Formulations for Finite Difference Linear Dynamic Analyses: Performance and Practical Recommendations,” *Computers and Geotechnics*, vol. 142, 2022. [[CrossRef](#)] [[Google Scholar](#)] [[Publisher Link](#)]
- [8] Rory Cordero, Gilberto Leiva, and Marcial Baeza, “Damage Analysis of a Reinforced Concrete Building in Santiago During the Earthquake of February 27, 2010,” *Works and Projects*, no. 35, pp. 65-75, 2024. [[CrossRef](#)] [[Google Scholar](#)] [[Publisher Link](#)]
- [9] Samaniego Palomino, Juan Diego Ricardo, “*Experimental Analysis of the Behavior of Reinforced Concrete Beams Strengthened with CFRP Strips under Quasi-Static Cyclic Reversed Actions*,” Master’s Thesis, Pontifical Catholic University of Peru, pp. 1-169, 2021. [[Google Scholar](#)] [[Publisher Link](#)]
- [10] Manuel Antonio Cando Loachamin, “*Effect of Stiffness on the Seismic Performance of Buildings Structured with Reinforced Concrete Walls*,” Doctoral Tesis, Pontifical Catholic University of Chile, 2020. [[Google Scholar](#)] [[CrossRef](#)] [[Publisher Link](#)]
- [11] Hao Jin et al., “Effect of Rubber Surface Treatment on Damping Performance of Rubber-Mortar ITZ in Rubberized Concrete,” *Journal of Building Engineering*, vol. 83, 2024. [[CrossRef](#)] [[Google Scholar](#)] [[Publisher Link](#)]
- [12] Payal Gwalani, and Yogendra Singh, “Performance-Based Seismic Design of RC Structures,” *Theory and Practice in Earthquake Engineering and Technology*, pp. 309-330, 2023. [[CrossRef](#)] [[Google Scholar](#)] [[Publisher Link](#)]
- [13] G.M. Calvi, M.J.N. Priestley, and M.J. Kowalsky, “Displacement-Based Seismic Design of Structures,” *Earthquake Spectra*, vol. 24, no. 2, 2008. [[CrossRef](#)] [[Google Scholar](#)] [[Publisher Link](#)]
- [14] A. Benavent-Climent, “Influence of Hysteretic Dampers on the Seismic Response of Reinforced Concrete Wide Beam–Column Connections,” *Engineering Structures*, vol. 28, no. 4, pp. 580-592, 2006. [[CrossRef](#)] [[Google Scholar](#)] [[Publisher Link](#)]
- [15] George A. Papagiannopoulos, “On the Modal Damping Ratios of Mixed Reinforced Concrete – Steel Buildings,” *Soil Dynamics and Earthquake Engineering*, vol. 178, 2024. [[CrossRef](#)] [[Google Scholar](#)] [[Publisher Link](#)]
- [16] Ragi Krishnan, and Vidhya Lakshmi Sivakumar, “Profound Impact of Shear Wall on Stability of Regular and Irregular Reinforced Concrete Structures – A Review,” *Materials Today: Proceedings*, 2023. [[CrossRef](#)] [[Google Scholar](#)] [[Publisher Link](#)]
- [17] Fernando Fuentes et al., “Determining the Dynamic Characteristics of a Multi-Story RC Building Located in Chile: A Comparison of the Results between the Nonparametric Spectral Analysis Method and the Parametric Stochastic Subspace Identification Method,” *Applied Sciences*, vol. 12, no. 15, pp. 1-20, 2022. [[CrossRef](#)] [[Google Scholar](#)] [[Publisher Link](#)]
- [18] Jorge Enrique Lucen Gómez, and Yerko Anthony Samokic Quiquia,, “*Comparative Structural Analysis and Design of a Ten-Story Reinforced Concrete Building with Fixed and Isolated Foundations*,” Thesis, Pontifical Catholic University of Peru, pp. 1-166, 2018. [[Google Scholar](#)] [[Publisher Link](#)]
- [19] Cinthia Raquel Soto Raico, and Anita Elizabet Alva Sarmiento, “Comparison of Seismic Analysis Using Different Percentages of Structural Damping,” *Latin American and Caribbean Consortium of Engineering Institutions*, pp. 1-8, 2022. [[CrossRef](#)] [[Publisher Link](#)]
- [20] Solorio Quintana et al., Experimental Determination of Structural Damping of a Masonry Building, Academia. [Online]. Available: [https://www.academia.edu/36510145/Determinaci%C3%B3n\\_experimental\\_del\\_amortiguamiento\\_estructural\\_de\\_un\\_Edificio\\_de\\_Ma\\_mposter%C3%ADa](https://www.academia.edu/36510145/Determinaci%C3%B3n_experimental_del_amortiguamiento_estructural_de_un_Edificio_de_Ma_mposter%C3%ADa)
- [21] Taehyu Ha, Seung-Hoon Shin, and Hongjin Kim, “Damping and Natural Period Evaluation of Tall RC Buildings Using Full-Scale Data in Korea,” *Applied Sciences*, vol. 10, no. 5, pp. 1-16, 2020. [[CrossRef](#)] [[Google Scholar](#)] [[Publisher Link](#)]
- [22] Francisco J. Pallarés et al., “Experimental and Analytical Assessment of the Influence of Masonry Façade Infills on Seismic Behavior of RC Frame Buildings,” *Engineering Structures*, vol. 235, 2021. [[CrossRef](#)] [[Google Scholar](#)] [[Publisher Link](#)]
- [23] Victor I. Fernandez-Davila, and Arnold R. Mendoza, “Damping Modification Factors for the Design of Seismic Isolation Systems in Peru,” *Earthquake Spectra*, vol. 36, no. 4, pp. 2025-2085, 2020. [[CrossRef](#)] [[Google Scholar](#)] [[Publisher Link](#)]
- [24] ETABS, Csiespana. [Online]. Available: <http://www.csiespana.com/software/5/etabs>

- [25] Ahed Habib, Umut Yildirim, and Ozgur Eren, “Seismic Behavior and Damping Efficiency of Reinforced Rubberized Concrete Jacketing,” *Arabian Journal for Science and Engineering*, vol. 46, pp. 4825-4839, 2021. [[CrossRef](#)] [[Google Scholar](#)] [[Publisher Link](#)]
- [26] Standard E.030 Seismic-resistant Design, National Building Regulations, pp. 1-81, 2020. [Online]. Available: <https://drive.google.com/file/d/1W14N6JldWPN8wUZSqWZnUphg6C559bi-/view>
- [27] Standard E.020 Loads, National Building Regulations, pp. 1-29, 2020. [Online]. Available: [https://drive.google.com/file/u/1/d/15atg-9w0OEXjR5C1m6IXUFihwYeUh1aN/view?usp=sharing&usp=embed\\_facebook](https://drive.google.com/file/u/1/d/15atg-9w0OEXjR5C1m6IXUFihwYeUh1aN/view?usp=sharing&usp=embed_facebook)
- [28] Emrah Erduran, “Evaluation of Rayleigh Damping and Its Influence on Engineering Demand Parameter Estimates,” *Earthquake Engineering & Structural Dynamics*, vol. 41, no. 14, pp. 1905-1919, 2012. [[CrossRef](#)] [[Google Scholar](#)] [[Publisher Link](#)]
- [29] Jonathan Pulido, Structural Dynamics, 4ed Anil K. Chopra, Academia, 2026. [Online]. Available: [https://www.academia.edu/36451323/Dinamica\\_de\\_Estructuras\\_4Ed\\_Anil\\_K\\_Chopra](https://www.academia.edu/36451323/Dinamica_de_Estructuras_4Ed_Anil_K_Chopra)
- [30] Koichi Morita, “Damping Ratio Estimation of an Existing 8-story Building Considering Soil-Structure Interaction Using Strong Motion Observation Data,” *Building Research Institute*, pp. 1-8, 2006. [[Google Scholar](#)] [[Publisher Link](#)]
- [31] Rafael Salinas-Basualdo, Mario E. Rodríguez, and y Roque A. Sánchez, “Vibrating Table Tests of Miniature Buildings with Conventional and Self-Centering Concrete Structural Walls,” *Seismic Engineering*, no. 89, pp. 101-134, 2013. [[Google Scholar](#)] [[Publisher Link](#)]
- [32] ASCE/SEI 7-22, “Front Matter for Minimum Design Loads and Associated Criteria for Buildings and Other Structures,” *Minimum Design Loads and Associated Criteria for Buildings and Other Structures*, pp. 1-60, 2021. [[CrossRef](#)] [[Google Scholar](#)] [[Publisher Link](#)]
- [33] P. Bisch et al., “Eurocode 8: Seismic Design of Buildings,” *Publications Office of the European Union*, 2012. [[Google Scholar](#)] [[Publisher Link](#)]
- [34] N. Nakamura et al., “Initial Damping Ratio for the Seismic Design of Buildings,” *17<sup>th</sup> World Conference on Earthquake Engineering*, Sendai, Japan, 2020. [[Google Scholar](#)] [[Publisher Link](#)]
- [35] Pengfei Ma, and Shangke Yuan, “Seismic Retrofitting of RC Frames Using Viscous Dampers: Numerical Simulation and Nonlinear Response Analysis,” *Infrastructures*, vol. 10, no. 9, pp. 1-18, 2025. [[CrossRef](#)] [[Google Scholar](#)] [[Publisher Link](#)]